CID Imaging - Present Status and Opportunities *

G.J. Michon
General Electric Co.
CR&D
Schenectady, NY

H.K. Burke
General Electric Co.
CR&D
Schenectady, NY

D.M. Brown
General Electric Co.
CR&D
Schenectady, NY

M. Ghezzo
General Electric Co.
CR&D
Schenectady, NY

ABSTRACT CID image sensors, which employ intra-cell transfer and injection to sense photon-generated charge at each image site, have evolved from relatively low density sequential-injection structures to high-speed, high-density arrays capable of non-destructive readout. A more recent readout method, termed Parallel Injection, separates the functions of signal charge detection and injection. The level of signal charge at each sensing site is detected during a line scan,and, during the line retrace interval, all charge in the selected line is injected. The injection operation is used to reset (empty) the charge storage capacitors after line readout has been completed. Non-destructive readout is possible by deferring the injection operation.

The parallel injection technique is well adapted to TV scan formats in that the signal is read out at high speed, line-by-line. A 244 line by 248 element TV-compatible imager employing this technique has been constructed and operation demonstrated.

An additional improvement in the CID structure has been the replacement of the opaque aluminum electrodes with transparent conductors. Devices fabricated in this way have achieved quantum efficiencies in the order of 70% over the spectral range of 4000A to 8000A; front illuminated.

The coincident voltage selection method is not constrained to sequential array scanning. Spiral, sub-raster, or "random" scanning can be implemented with appropriate row and column selection circuitry. The capability of repeated readout, during or subsequent to exposure, allows a number of system functions not previously possible. Time exposures can be monitored via NDRO and terminated when the desired information has been acquired. Signal-to-noise performance can also be improved through repeated readout of a stored image.

INTRODUCTION

In contrast to CCD imagers, in which the signal charge is transferred to the edge of the array for sensing, the CID approach confines this charge to the site during sensing. Site addressing is done by an X-Y, coincident voltage technique, not unlike that used in digital memory structures. In the basic structure, readout is effected by injecting the charge from individual sites into the substrate and detecting the resultant displacement current. A number of variations of this technique are possible, some of which will be described below. In this paper we describe the basic CID structure, several site selection and readout techniques, and CID fabrication methods. Performance data for various CID structures are given and discussed.

* CID imager development was sponsored in part by the United States Army Electronics Command, Night Vision Laboratory, the Advanced Research Projects Agency (ARPA) and the Air Force Systems Command, United States Air Force.

BASIC DESCRIPTION

CHARGE INJECTION

The CID imaging technique requires that the collected photon-generated charge be ultimately disposed of by injection into the substrate. Upon injection, this charge must either recombine or be collected to avoid interference with subsequent readouts. For the high-lifetime material usually required for image sensors, recombination is not a suitable method of charge disposition, since re-collection of this charge can give rise to objectionable image lag and crosstalk. For this reason, most CID imagers are fabricated on epitaxial material. The epitaxial junction, which underlies the imaging array, acts as a buried collector for the injected charge. If the thickness of the epitaxial layer is comparable to the spacing between sensing sites, almost all of the injected charge will be collected by the reverse biased epitaxial junction and injection crosstalk is avoided. The time required for charge injected at the surface to be removed from the epitaxial layer has been determined analytically and experimentally to be approximately 100 nsec for the conditions typically used in the CID. The effective thickness of the epitaxial layer can be adjusted during operation by varying the junction bias voltage.

The use of the buried charge collector also modifies the spectral response and MTF characteristics in a manner that will be described below.

For intensified applications, where it is required to thin the silicon substrate for backside illumination by electrons, the epitaxial structure can be replaced by charge collectors on the front surface. These take the form of a grid of diffused conductors separating the rows and columns. CID imagers operated in this fashion exhibit injection characteristics quite similar to epitaxial devices.

SEQUENTIAL INJECTION

An array designed for sequential injection which includes integral scanning shift registers is diagrammed in Fig. 1 (a). Each sensing site consists of two MOS capacitors with their surface inversion regions coupled such that charge can readily transfer between the two storage regions. A large voltage is applied to the row-connected electrodes so that photon-generated charge collected at each site is stored under the row electrode, thereby minimizing the capacitance of the column lines. The sensing site cross-sections, Fig. 1 (b), illustrate the silicon surface potentials and locations of stored charge under various applied voltage conditions.

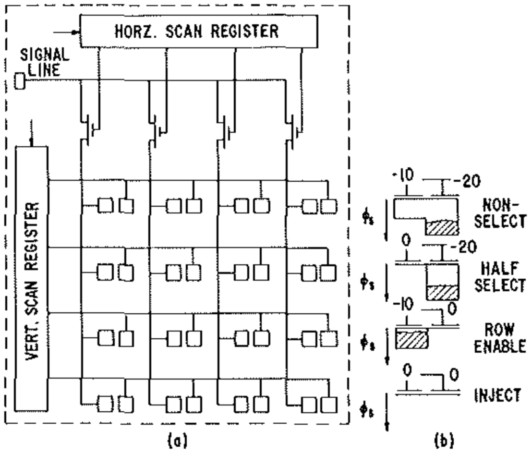

Fig. 1 Basic accessing scheme, (a) schematic diagram of array, (b) sensing site cross-section showing silicon surface potentials and charge locations.

A line is selected for readout by setting its voltage to zero by means of the vertical scan register. Signal charge at all sites of that line is transferred to the column capacitors, corresponding to the Row Enable condition shown in Fig. 1 (b). The charge is then injected by driving each column voltage to zero, in sequence, by means of the horizontal scan register and the signal line. The basic signal is contained in the majority-carrier displacement current that flows upon injection of the stored charge. This signal can be detected anywhere in the loop composed of the substrate, driver circuit, and the driven array lines. In general, the array lines provide the lowest capacitance environment for signal detection. Charge in the unselected lines remains under the row-connected electrodes during the injection pulse time (column voltage pulse). This corresponds to the half select condition of Fig. 1 (b).

This readout method has been termed "sequential injection" since, regardless of the scan geometry, the charge at the storage sites is injected in time sequence.

PARALLEL INJECTION

In this readout technique, the functions of signal charge detection and injection are separated. The level of signal charge at each sensing site is detected by intracell transfer during a line scan and, during the line retrace interval, all charge in the selected line can be injected.

A diagram of 4 X 4 array designed for parallel injection is illustrated in Fig. 2 with the relative silicon surface potentials and signal charge locations included. As before, the voltage applied to the row electrodes is larger than that applied to the column electrodes to prevent the signal charge stored at unaddressed locations from affecting the column lines. At the beginning of a line scan, all rows have voltage applied and the column lines are reset to a reference voltage, V_s, by means of switches S_1 through S_4 and then disconnected. Voltage is removed from the line selected for readout (X_3 in Fig. 2) causing the signal charge at all sites of that line to transfer to the column electrodes. The voltage on each floating column line changes by an amount equal to the signal charge divided by the column capacitance. The horizontal scanning register is then operated to scan all column voltages and deliver the video signal to the on-chip preamplifier, Q_1. The input voltage to Q_1 is reset to a reference level prior to each step of the horizontal scan register.

At the end of each line scan all charge in the selected line can be injected simultaneously by driving all column voltages to zero through switches S_1 through S_4. Alternatively, the injection operation can be omitted and voltage reapplied to the row after readout causing the signal charge to transfer back under the row electrodes. This action retains the signal charge and constitutes a nondestructive readout operation.

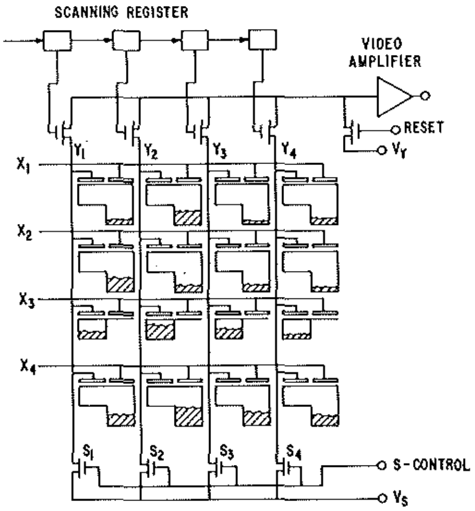

Fig. 2 Schematic diagram of a CID array designed for parallel-injection readout. Surface potentials and charge locations are included.

The parallel injection approach permits high speed readout and is thus well adapted to TV-scan formats, and offers optional nondestructive readout. A 244 line by 248 element imager, employing this technique and including an on-chip preamplifier, has been designed, fabricated, and evaluated in both the normal and nondestructive readout mode.

For TV-compatible operation, a line time interval of 63 micro seconds (5 MHz element rate) is used and the vertical scan rate is 60 scans per second. The image is completely read out during each interlaced field of the standard TV frame such that video is displayed on all 488 active lines of the 525 line system.

ARRAY FABRICATION

To date, most CID imagers have been fabricated with a p-channel, silicon-gate process modified to provide a top contact to the epitaxial layer. The disadvantages of this method are requirements for a diffused area and an interlevel contact at each sensing site. This results in some signal degradation as well as an area penalty. Both of these problems have been overcome by a design which employs an overlapping-electrode structure for charge transfer. This technique is now being used to make high-density CID imagers. This method permits simultaneous fabrication of active devices for array scanning and can include highly transparent upper-level electrodes for improved spectral sensitivity (1).

PERFORMANCE

SENSITIVITY

Sensitivity as a function of wavelength for both the bulk and pitaxial 100 X 100 structures is plotted in Fig. 3 (lower curves). The sensitivity of the epitaxial structure is about half that of the bulk imager in the visible region of the spectrum. This sensitivity reduction reflects collection by the epitaxial junction of some of the signal charge generated in the space between sensing sites. Thus, some of the indicated sensitivity loss is not a real loss in that it represents loss of charge that was contributing to cross talk in the bulk sample. The somewhat greater loss in the infrared region is to be expected because of the deeper photon penetration at these wavelengths.

The upper curve shows the sensitivity improvement resulting from the use of a highly transparent material for the upper level in an overlapping electrode configuration. Since this data was taken using a bulk imager, it should be compared to a standard bulk results (middle curve). Of particular significance is the greatly increased blue response which results from the substitution of the transparent material for a large portion of the polysilicon gate-electrode material.

BLOOMING

The CID structure is resistant to image blooming since each sensing site is electrically isolated from its neighbors. Charge spreading in the substrate is minimized by the underlying charge collector.

In sequential injection, blooming of the displayed image occurs if charge is injected from a half-selected site during readout of another site on the same column. This excess injected charge is detected as signal and adds to the displayed video. This results in brightening of the affected column upon overload of a single site.

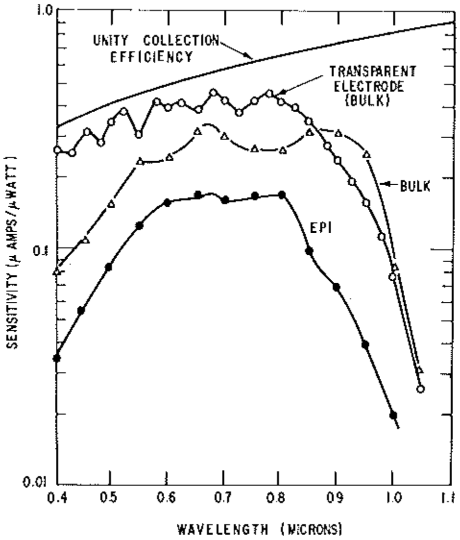

Fig. 3 Sensitivity as a function of wavelength of incident radiation.

The image displayed in the parallel injection approach exhibits relatively little blooming as a result of sensing site overload. This is because the half-select and injection operations occur during the horizontal blanking interval. While excess charge can accumulate during a line scan interval and cause column brightening for overloads occurring in the right-hand portion of the image field, this effect is attenuated by the line-to-frame integration time ratio.

For NDRO operation, virtually no blooming occurs, since the charge is not injected. The affected sites fill to capacity and cease collecting charge. In all cases, radial spreading of excess charge is prevented by the underlying charge collector.

The image shown in the photograph, Fig. 4 was produced by a 244 X 188 CID imager exposed to a high contrast scene. This particular camera uses a modified parallel injection readout method that is highly resistent to image blooming, as indicated by the image of the automobile head lamps.

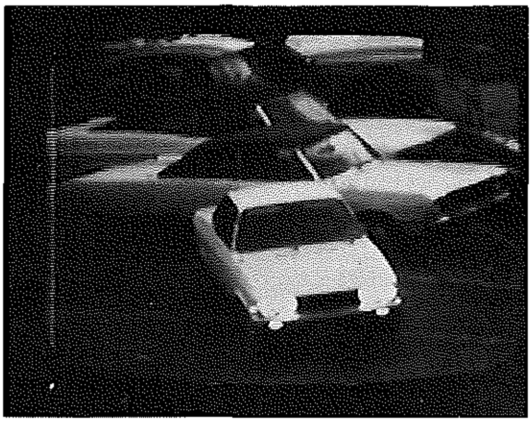

Fig. 4 CID image of high-contrast scene.

MODULATION TRANSFER FUNCTION

Since each sensing site is electrically isolated from adjacent sites, the MTF of CID imagers is intrinsically quite high. This electrical isolation is maintained for both the charge collection and readout operations; the epitaxial charge collector inhibits charge migration in the substrate, and there is no MTF loss effects due to site-to-site transfer during readout. Imagers made on high-lifetime bulk material do exhibit loss of MTF to a degree dependent on the carrier lifetime of the particular material used. Image lag would occur in a like fashion. Since the use of an epitaxial collector reduces the measured sensitivity, particularly for the longer wavelengths, a trade-off situation exists in the design of the structure. By adjusting the epitaxial thickness with relation to the site separation, these two performance characteristics can be tailored to a particular application. The sensitivity loss of the epitaxial structure in the 100 X 100 imager, as shown in Fig. 3, illustrates this effect. In this case, epitaxial thickness is small compared to the site separation, resulting in about a two-to-one loss in measured sensitivity. This same imager exhibits an in-phase MTF of nearly 100% at the Nyquist limit.

NOISE SOURCES

The primary temporal noise sources in CID imagers are amplifier noise, capacitor-reset (KTC) noise, and bias charge shot noise. Unlike the CCD, the CID has negligible charge transfer noise. The capacative load seen by the signal charge can be reduced by the use of an on-chip MOSFET as the first stage of the video amplifier. This device should have high transconductance for reduced Johnson noise (2) and a large channel area for reduced 1/f noise (3). In most applications 1/f noise is not a serious problem since correlated double sampling can be used to attenuate noise components that are lower in frequency than the sampling rate. This technique also eliminates KTC noise in many cases. In the parallel injection readout method, the column reset switches introduce KTC noise that is not rejected by correlated double sampling.

Theoretical amplifier noise levels are on the order of a few hundred carriers in the CID, while KTC noise can be negligible or the predominant noise source, depending on the specific array design and readout method. Noise in the bias charge can be of the same order as amplifier noise.

DARK CURRENT

A critical performance factor in image sensors is the magnitude of thermally generated charge, commonly called dark current. In addition to reducing charge storage capacity, dark current limits integration time, and can contribute to undesirable background patterns in the displayed image. Random fluctuations in the dark current contribute to system noise. While cooling the sensor can reduce dark current, the additional system complexity is not desirable for most system applications.

In the CID, significantly more silicon area can be used for photon charge generation than for charge storage and readout. Since the charge generation rate in non-depleted bulk silicon is orders of magnitude less than in depleted silicon (4) the CID collects photon-generated charge from virtually the entire site area while generating dark only in the storage area.

CID arrays are operated with a bias voltage somewhat higher than the threshold voltage to allow the accumulation of a bias charge in the storage area. This inhibits charge pumping losses during readout and also results in an additional reduction in dark current, since surface leakage is much smaller under inversion conditions than under depleted conditions (5).

Thermal charge generation rates in a typical 100 X 100 CID imager for various operating conditions are shown in Fig. 5. Mimimum dark current results from biasing the storage electrodes such that charge is stored under both electrodes, Fig. 5(a). If one of the storage regions is operated in depletion, the increased surface leakage in this region results in a higher dark current, as shown in Fig. 5(b). The effect of temperature on charge generation rate is also shown in Fig. 5. A reduction in temperature of twenty degrees Celsius results in a tenfold decrease in the rate of charge accumulation. This relationship has been found to hold over a wide range of temperatures and amounts to a two-to-one change in charge buildup for each six-degree change in temperature.

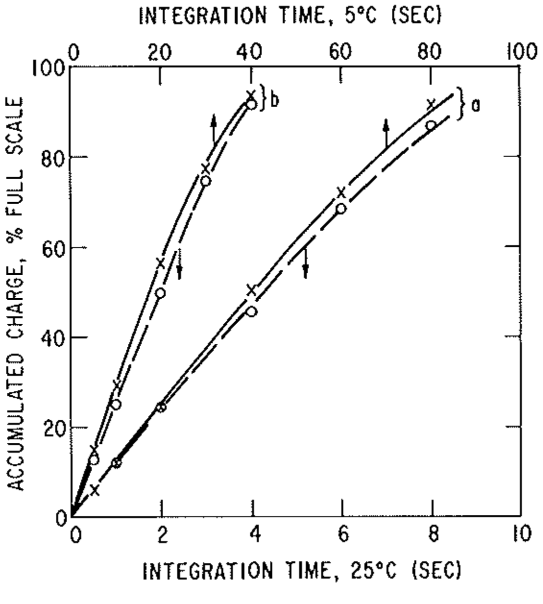

Fig. 5 Thermal charge buildup as a function of time and temperature, with a) both storage regions inverted, and b) one region depleted.

OTHER FEATURES

RANDOM SELECTION

Certain imaging applications, such as those involving bandwidth compression, could be much more effectively implemented if the primary image information could be made available in other than the progressive scan format employed by most currently available imaging devices. The X-Y, coincident voltage configuration of the CID makes it easily adaptable to special scan formats, including "random" addressing, in which each sensing site can be addressed without regard to its time or spatial sequence with respect to other sites in the array. In many respects, image site selection in the CID resembles MOS memory selection, and many of the decoding techniques developed for these memories could be applied to random access imagers. Charge could be injected during readout in the manner of sequential injection or deferred to a later time as is done in parallel injection. Charge integration time could be held constant for all sites in the array by having the site selection pattern repeat frame-to-frame, or, conversely, the integration time for particular sites could be tailored to local scene brightness.

NONDESTRUCTIVE READOUT

The nondestructive charge readout technique of Tiemann, et al (6), can be effectively applied to CID imagers. This fact, combined with low dark current performance, make image storage in the CID array a practicality. To demonstrate this, a cooled 244 X 248 CID imager has been operated in a nondestructive readout mode for three hours at 30 frames/second with no apparent degradation of the stored image other than a slight increase in background charge. The charge loss during this experiment was estimated to be much less than one carrier per pixel per frame.

In a second experiment, a series of exposures was made at successively lower light levels while operating at 30 frames/second, NDRO. The time to reach a given level of signal was recorded for each exposure. Exposure time was found to be inversely proportional to light intensity with no measurable reciprocity loss down to light levels in the order of two carriers per pixel per frame.

CONCLUSIONS

The CID approach leads to many desirable performance characteristics, including high sensitivity over a wide spectral range, low dark current, high MTF, and resistance to blooming -- in a structure that is tolerant to defects and permits many design options such as nondestructive readout and random scanning. On balance, these features more than compensate for its relatively high thermal noise level as compared to that reported for other approaches,

ACKNOWLEDGMENT

The authors would like to acknowledge the contributions of K. Keller, D. Meyer, and P. Salvagni for sensor fabrication; and S. Dworak for test circuit fabrication and device evaluation.

BIBLIOGRAPHY

(1) D.M. Brown, M. Ghezzo, and M. Garfinkel, "Transparent Metal Oxide Electrode CID Imaging Array", ISSCC Digest of Technical Papers, Feb. 1975, pp. 34-35.

(2) van der Ziel, A., "Thermal Noise in Field Effect Transistors", Proc. IEEE, 50, 8, (August 1962), pp. 1808-1812).

(3) S. Christensson, L. Lundstrom, and C. Svensson, "Low Frequency Noise in MOS Transistors", Solid-State Electronics, Vol 11, p. 797-812 (1968).

(4) A.S. Grove, "Physics and Technology of Semiconductor Devices", John Wiley and Sons, 1967, pp. 298-302.

(5) D.G. Ong and R.F. Pierret, "Thermal Carrier Generation in Charge-Coupled Devices" IEEE Trans. on Electron Devices, ED-22, 593-602, (August 1975).

(6) J.J. Tiemann, W.E. Engeler, R.D. Baertsch, and D.M. Brown, "Intracell Charge Transfer Structures for Signal Processing", IEEE Trans. on Electron Devices, ED-21, pp. 300, (1974).